Journal of Structural Engineering

Modeling the Coupling Effect of CLT Connections under Bi-axial Loading

--Manuscript Draft--

Manuscript Number:	STENG-7803R2
Full Title:	Modeling the Coupling Effect of CLT Connections under Bi-axial Loading
Manuscript Region of Origin:	CANADA
Article Type:	Technical Paper
Section/Category:	Wood Structures
Funding Information:	Canadian Network for Research and Innovation in Machining Technology, Natural Sciences and Engineering Research Council of Canada — Not applicable
Abstract:	This paper presents the modeling of coupling effect of tension and shear loading on Cross Laminated Timber (CLT) connections using a finite element based algorithm called HYST. The model idealizes the connections as a "Pseudo Nail" - elastoplastic beam elements (the nail) surrounded by compression-only spring elements (steel sheath and wood embedment). A gap size factor and an unloading stiffness degradation index of the spring elements under cyclic loading were integrated into the optimized HYST algorithm to consider the coupling effect. The model was calibrated to compare with 32 configurations of CLT angle bracket and hold-down connections tests: in tension with co-existent constant shear force, and in shear with co-existent tension force. The results showed that the proposed model can fully capture the coupling effect of typical CLT connections, considering strength degradation, unloading and reloading stiffness degradation, and pinching effect. The model provided a useful tool for nail-based timber connections and a mechanism-based explanation to understand the hysteretic behaviour of CLT connections under bi-axial loading.
Corresponding Author:	Jingjing Liu, PhD Vancouver, CANADA
Corresponding Author E-Mail:	jingjing.liu88@gmail.com
Order of Authors:	Jingjing Liu, PhD Frank Lam Ricardo O. Foschi Minghao Li
Suggested Reviewers:	Mingjuan He, PhD Professor, Tongji University Professor He is an expert in wood science and computational mechanics. Hyungsuk Thomas Lim, PhD Assistant Professor, Mississippi State University Professor Lim is an expert in wood mechanics and CLT connections.
Opposed Reviewers:	
Additional Information:	
Question	**Response**
Authors are required to attain permission to re-use content, figures, tables, charts, maps, and photographs for which the authors do not hold copyright. Figures created by the authors but previously	No

published under copyright elsewhere may require permission. For more information see http://ascelibrary.org/doi/abs/10.1061/9780784479018.ch03. All permissions must be uploaded as a permission file in PDF format. Are there any required permissions that have not yet been secured? If yes, please explain in the comment box.	
ASCE does not review manuscripts that are being considered elsewhere to include other ASCE Journals and all conference proceedings. Is the article or parts of it being considered for any other publication? If your answer is yes, please explain in the comments box below.	No
Is this article or parts of it already published in print or online in any language? ASCE does not review content already published (see next questions for conference papers and posted theses/dissertations). If your answer is yes, please explain in the comments box below.	No
Has this paper or parts of it been published as a conference proceeding? A conference proceeding may be reviewed for publication only if it has been significantly revised and contains 50% new content. Any content overlap should be reworded and/or properly referenced. If your answer is yes, please explain in the comments box below and be prepared to provide the conference paper.	Yes
If your answer is yes, please explain in the comments box below and be prepared to provide the conference paper. as follow-up to "Has this paper or parts of it been published as a conference proceeding? A conference proceeding may be reviewed for publication only if it has been significantly revised and contains 50% new content. Any content overlap should be reworded and/or properly referenced. If your answer is yes, please explain in the comments box below and be prepared to provide the conference paper.	20% of the paper was published in WCTE2016 with the title of "Experimental test of cross laminated timber connections under bi-directional loading". However, this part was briefly introduced to validate the numerical model with experimental data.

"	
ASCE allows submissions of papers that are based on theses and dissertations so long as the paper has been modified to fit the journal page limits, format, and tailored for the audience. ASCE will consider such papers even if the thesis or dissertation has been posted online provided that the degree-granting institution requires that the thesis or dissertation be posted. Is this paper a derivative of a thesis or dissertation posted or about to be posted on the Internet? If yes, please provide the URL or DOI permalink in the comment box below.	No
Each submission to ASCE must stand on its own and represent significant new information, which may include disproving the work of others. While it is acceptable to build upon one's own work or replicate other's work, it is not appropriate to fragment the research to maximize the number of manuscripts or to submit papers that represent very small incremental changes. ASCE may use tools such as CrossCheck, Duplicate Submission Checks, and Google Scholar to verify that submissions are novel. Does the manuscript constitute incremental work (i.e. restating raw data, models, or conclusions from a previously published study)?	No
Authors are expected to present their papers within the page limitations described in <u><i>Publishing in ASCE Journals: A Guide for Authors</u></i>. Technical papers and Case Studies must not exceed 30 double-spaced manuscript pages, including all figures and tables. Technical notes must not exceed 7 double-spaced manuscript pages. Papers that exceed the limits must be justified. Grossly over-length papers may be returned without review. Does this paper exceed the ASCE length limitations? If yes, please provide justification in the comments box below.	No
All authors listed on the manuscript must have contributed to the study and must	No

approve the current version of the manuscript. Are there any authors on the paper that do not meet these criteria? If the answer is yes, please explain in the comments.	
Was this paper previously declined or withdrawn from this or another ASCE journal? If so, please provide the previous manuscript number and explain what you have changed in this current version in the comments box below. You may upload a separate response to reviewers if your comments are extensive.	No
Companion manuscripts are discouraged as all papers published must be able to stand on their own. Justification must be provided to the editor if an author feels as though the work must be presented in two parts and published simultaneously. There is no guarantee that companions will be reviewed by the same reviewers, which complicates the review process, increases the risk for rejection and potentially lengthens the review time. If this is a companion paper, please indicate the part number and provide the title, authors and manuscript number (if available) for the companion papers along with your detailed justification for the editor in the comments box below. If there is no justification provided, or if there is insufficient justification, the papers will be returned without review.	
If this manuscript is intended as part of a Special Issue or Collection, please provide the Special Collection title and name of the guest editor in the comments box below.	
Recognizing that science and engineering are best served when data aremade available during the review and discussion of manuscripts andjournal articles, and to allow others to replicate and build on workpublished in ASCE journals, all reasonable requests by reviewers formaterials, data, and associated protocols must be fulfilled. If you are restricted from sharing your data and materials, please explain below.	
Papers published in ASCE Journals must	The manuscript is the first to systematically examine the behaviour of CLT connections

make a contribution to the core body of knowledge and to the advancement of the field. Authors must consider how their new knowledge and/or innovations add value to the state of the art and/or state of the practice. Please outline the specific contributions of this research in the comments box.	under bi-axial loading through robust experimental setup, mechanism-based model and detailed parameter study. It gives a more profound understanding of the structural behaviour of the CLT connecters through tests and numerical simulation of CLT connections under bi-axial loading.
The flat fee for including color figures in print is $800, regardless of the number of color figures. There is no fee for online only color figures. If you decide to not print figures in color, please ensure that the color figures will also make sense when printed in black-and-white, and remove any reference to color in the text. Only one file is accepted for each figure. Do you intend to pay to include color figures in print? If yes, please indicate which figures in the comments box.	No
If there is anything else you wish to communicate to the editor of the journal, please do so in this box.	

Modeling the Coupling Effect of CLT Connections under Bi-axial Loading

Jingjing Liu[1]; Frank Lam[2]; Ricardo O. Foschi[3]; and Minghao Li[4]

Abstract

This paper presents the modeling of coupling effect of tension and shear loading on Cross Laminated Timber (CLT) connections using a finite element-based algorithm called HYST. The model idealizes the connections as a "Pseudo-nail" - elastoplastic beam elements (the nail) surrounded by compression-only spring elements (steel sheath and wood embedment). A gap size factor and an unloading stiffness degradation index of the spring elements under cyclic loading were integrated into the optimized HYST algorithm to consider the coupling effect. The model was calibrated to compare with 32 configurations of CLT angle bracket and hold-down connections tests: in tension with co-existent constant shear force, and in shear with co-existent tension force. The results showed that the optimized model can fully capture the coupling effect of typical CLT connections, considering strength degradation, unloading and reloading stiffness degradation, and pinching effect. The model provided a useful tool for nail-based timber connections and a mechanism-based explanation to understand the hysteretic behaviour of CLT connections under bi-axial loading.

Keywords: CLT connection; coupling effect; bi-axial loading; degradation; modeling

[1] PhD, Department of Wood Science, University of British Columbia, 2424 Main Mall, BC, V6T1Z4, Vancouver, Canada (corresponding author). E-mail: jingjing.liu@alumni.ubc.ca
[2] Professor, Department of Wood Science, University of British Columbia, 2424 Main Mall, BC, V6T1Z4, Vancouver, Canada.
[3] Professor Emeritus, Department of Civil Engineering, University of British Columbia, 6250 Applied Science Lane, BC, V6T1Z4, Vancouver, Canada.
[4] Senior Lecturer, Civil and Natural Resources Engineering, University of Canterbury, 69 Creyke Road, Christchurch, New Zealand.

Introduction

In the past decades, Cross Laminated Timber (CLT) has been widely used as load bearing components such as walls and floors due to its high stability and load capacity. Many experimental tests have been conducted on CLT structural performance (Dujic *et al*. 2005, 2006, 2008; Ceccotti *et al*. 2006, 2008, 2013; Popovski *et al*. 2010, 2015; Pei *et al*. 2013, 2014, 2016; Ganey 2015; van de Lindt *et al.* 2019). Those tests revealed that the connections anchoring CLT panels with foundations and walls are the critical elements that govern the structural response. The non-linearity of the connection is the key importance to design safe CLT structures. For those connections, one typical assumption is that, hold-downs take the tension force to resist overturning moment, while angle brackets take the shear force to resist the lateral force. Under such assumptions, several CLT connections have been tested for monotonic and cyclic tests, all loaded in only one direction (Rinaldin *et al*. 2013; Schneider *et al*. 2013; Tomasi and Smith 2014; Mahdavifar *et al.* 2018a).

However, recent tests of CLT panels under cyclic loading demonstrated that both hold-downs and angle brackets undertake uplift and slip resistances (Gavric *et al*. 2011). Moreover, those forces are coupled on the connections, which deteriorate their mechanical properties and seismic capacity, questioning the safety and rationality of current design methods. To investigate such coupling effect, monotonic and cyclic tests of CLT connections have been conducted under co-existent shear and tension load (Liu and Lam 2016, 2018, 2019; Pozza *et al*. 2017).

As for numerical models, two main approaches have been proposed to investigate the nonlinearity of CLT connections under different loading protocols. The first approach is to consider the CLT connection as a macro element (Folz and Filiatrault 2001; Pozza et al. 2009; Fragiacomo et al. 2011; Ceccotti et al. 2013; Rinaldin et al. 2013; Shen et al. 2013; Lowes et al.

2004; Liu and Lam 2014; Zhang et al. 2015; Pozza et al. 2017; Mahdavifar *et al.* 2018b). Those models have limitations and inherent uncertainties in their applicability to other protocols, and in particular, to seismic loading. It is recognized that shear wall response in cyclic loading depends on test protocols. Although those models can be fitted quite accurately to specific loops from cyclic loading, yet it is questionable whether the fitted curves would provide a good representation of CLT connections under other loading protocols. Besides, these models can be put into applications but provide little explanation in understanding the fundamental mechanism of CLT connections under complex loading.

The second approach is using mechanism-based micro elements to consider CLT connections. Because the behavior of a CLT connection is mostly governed by the behavior of nail connections, the hysteretic response from a CLT connection and that from a nail connection show strong similarity in characteristics of strength/stiffness degradation and pitching effect. Hence, the connection can be modeled as if it was a single nail connection (i.e, a pseudo-nail) (Gu and Lam 2004). Using this pseudo-nail approach, Li and Lam (2009) studied the diagonal-braced timber walls, Li *et al*. (2009) studied the seismic reliability of diagonal-braced walls and structural-panel-sheathed walls, and Li *et al*. (2014) studied the seismic performance of timber-steel hybrid structures. In this approach, the nonlinear behaviour of connections and walls are predicting through nonlinear analysis conducted at the fasteners level using the HYST algorithm. As a Finite Element detailed nail model, this algorithm can capture the hysteresis behaviour of timber connections using metal fasteners, which is based on the basic elastoplastic stress-strain relationship of the connector material and a simple presentation of the nonlinear behaviour of wood embedment medium. This approach has the advantage of being based on equivalent mechanical properties of the nail fasteners, steel plates, and the surrounding wood medium of a connection or wall, which helps understand the mechanism under complex loading through physical meanings.

The original HYST algorithm was proposed and adopted to calculate the hysteretic behavior of timber connections using metal fasteners (Foschi and Yao 2000). Li *et al*. (2011) modified this algorithm to improve its representation of strength and stiffness degradation. Key features of the improved algorithm include automatically tracking the formation of gaps between the nail and the wood, and strength degradation and reloading stiffness degradation of the wood embedment. Later on, Lim *et al*. (2017) modified the algorithm and embedded a more mechanistically sound withdrawal model with consideration of the displacement compatibility between the movement of the nail and the resisting wood medium.

In this paper, a gap size factor and an unloading stiffness degradation index are introduced into the HYST algorithm to fully address the hysteresis behaviour of CLT connections under bi-axial loading, which provides sufficient explanation of the coupling effect. First, it discusses the optimized model. Then the experimental tests of CLT connections under bi-axial loading are described. The paper subsequently presents modeling the hysteresis behaviour of the 32 configurations using the pseudo-nail model with the optimized HYST algorithm and discusses the parameters in the models.

Modeling Approach

The CLT connections under bi-axial loading were simulated as pseudo-nail models using HYST algorithm to consider the coupling effect. As a micro modeling approach, the pseudo-nail model has three parts: the nail, the sheath, and the wood embedment, which can represent the group of nails, the steel plate of hold-down/angle bracket, and the CLT wood panel in CLT connections, respectively. The HYST algorithm was modified to add features to characterize the strength degradation, unloading stiffness degradation, reloading stiffness degradation, and pinching effect of typical timber connections. Details about the model and algorithms are described as below. The original HYST algorithm can be found in Foschi *et al.* (2000) and the modified HYST algorithm can be found in Li *et al.* (2011).

Pseudo-nail model

The shapes of the load deformation curve of individual nail and that of connectors with fasteners have many similarities. The similarities can be explained since the structural response of CLT connections is governed by the characteristics of the nails. The effect of the deformations from all nails is imposed together to exhibit an overall load-displacement curve for CLT connections. Thus, it is possible to represent a CLT connection with mechanics-based analog as a single pseudo-nail. Fig. 1 (a) shows the nail connector model. Given a lateral force F to the covering sheath, the nail will have a displacement of Δ at the head of the nail. Meanwhile, the shank of the nail performed non-linear deformation in the surrounding wood embedment. Fig. 1 (b) and Fig. 1 (c) present angle bracket connection and hold-down connection as a pseudo-nail, respectively. The steel plate of angle bracket/hold-down is considered as the equivalent sheath. All nails are grouped as one pseudo-nail and CLT panel is considered as the equivalent wood embedment.

Fig. 1. (a) nail connector model; (b) pseudo-nail model of angle bracket connection; (c) pseudo-nail model of hold-down connection

Optimized HYST algorithm

From CLT connections under bi-axial loading experiments, it was found that due to the co-existent force in the perpendicular direction, the nails travelling in the gap encountered resistance. As shown in Fig. 2 (a), when there is only shear force applied, the nail can travel in the gap with no resistance. But with co-existent tension force applied (Fig. 5 (b)), such tension force caused pressure on the nail shank from surrounding wood embedment. This pressure provides lateral resistance to the nail in the gap during unloading. Furthermore, higher level of co-existent force caused larger resistance during unloading.

Fig. 2. Schematic section views of nails in the wood embedment: (a) nail movement under shear force with no co-existent tension load; (b) nail movement under shear force with co-existent tension load

To address such coupling effect, in the optimized HYST algorithm, a gap size factor β and an unloading stiffness degradation index γ were introduced into the modified HYST algorithm. The optimized algorithm can capture all features of nail-based connections under complex loading, including the strength degradation, reloading stiffness degradation, unloading stiffness degradation, and pinching effect. Table 1 shows the descriptions of the eight parameters to define this force-displacement relationship.

Table 1. Descriptions of embedment property parameters in optimized HYST algorithm

In the optimized HYST algorithm, the relationship between the pressure $p(w)$ and the deformation of sheath and wood embedment w in the embedment properties is shown in Fig. 3. It was noted that in CLT connections under bi-axial loading, the backbones of force-displacement curves also changed. This can be modeled by the change of embedment property parameters of equivalent wood embedment.

Fig. 3. Embedment properties in the optimized HYST algorithm

The displacement w starts at O with an initial stiffness of K_0. It reaches peak value P_{max} at D_{max} along the first exponential curve. After that, it follows the second exponential curve with a softening trend to Z. The backbone force-displacement curve is represented in Eq. (1).

$$\begin{cases} p(w) = (Q_0 + Q_1 w)(1 - e^{-K_0/Q_0}) & \text{if } w \le D_{max} \\ p(w) = P_{max} e^{Q_3 (w - D_{max})^2} & \text{if } w > D_{max} \end{cases} \quad (1)$$

where $P_{max} = (Q_0 + Q_1 D_{max})(1 - e^{-K_0 D_{max}/Q_0})$ and $Q_3 = \log(0.8)/[(Q_2 - 1.0)D_{max}]^2$.

When unloading from point A, instead of following a straight line with an unloading stiffness of K_0 in the original HYST algorithm and modified HYST algorithm, the unloading curve follows another straight line with an unloading stiffness of K_{UL} until it reaches point B. Point B is inside of the gap D_0, which indicates the contribution of resistance during unloading. When reloading from point B, the reloading stiffness K_{RL} is the same as the modified HYST algorithm. It is assumed that reloading from point B follows another straight line with reduced stiffness K_{RL} to point C. Subsequent unloading from point C will follow the original stiffness K_0 until D' is reached, resulting a new gap of magnitude D_0'. A reloading degradation index α is used to consider both the strength degradation and reloading stiffness degradation. The value of α is between 0 and 1. The reloading stiffness K_{RL}, which is related to the initial stiffness K_0 and the gap size D_0, is represented in Eq. (2).

$$\begin{cases} K_{RL} = K_0 & \text{if } D_0 \le D_y \\ K_{RL} = (D_y / D_0)^{\alpha} K_0 & \text{if } D_0 > D_y \end{cases} \quad (2)$$

where $D_y = Q_0 / (K_0 - Q_1)$, corresponding to a yielding deformation given by the intersection of the original slope and the asymptote.

The optimized algorithm introduced a gap size factor β to indicate the position of point B. The distance L_{OB} between point O and point B is calculated as $L_{OB} = \beta D_0$. An unloading degradation index γ is used to consider the unloading stiffness degradation. The value of γ is between 0 and 1. The unloading stiffness K_{UL}, which is related to the initial stiffness K_0, the gap size D_0, and the stiffness and reloading degradation index α, is represented in Eq. (3).

$$\begin{cases} K_{UL} = K_0 \quad \text{if } D_0 \le D_y \\ K_{UL} = (D_y / D_0)^{\alpha\gamma} K_0 \quad \text{if } D_0 > D_y \end{cases} \tag{3}$$

Where $D_y = Q_0 / (K_0 - Q_1)$, corresponding to a yielding deformation given by the intersection of the original slope and the asymptote.

The optimized algorithm has been compiled using the Fortran compiler in Intel Parallel Studio XE 2018. For the longest duration of protocol in the tests, which is the shear cyclic test of hold-down connections under co-existent tension force, it takes approximately 20 seconds to run on a computer with a quad-core CPU and 8 GB memory.

Parameter study

To understand the effect of the two introduced parameters and provide calibration methods for CLT connection modelling, a parameter study of the gap size factor β and the unloading degradation index γ on was carried out.

A trail model was established for a cyclic test. Four different values of gap size factor β, namely, 1, 0.8, 0.5, and 0, were input into this model while the remaining parameters were retained as initialled. The hysteresis loops are shown in Fig. 4. It was observed that, as the gap size factor decreased, first, the maximum loading capacity slightly increased. Second, the unloading path from the maximum load to 0 kN force changed significantly. Third, the slipping distance between 0 mm displacement and the displacement where the force was unloaded to 0 kN decreased. Finally, the degradation effect was weakened.

Fig. 4. Hysteresis loops with different gap size factors: (a) 1.0; (b) 0.8; (c) 0.5; (d) 0

Four different values of unloading degradation index γ, namely, 0, 0.2, 0.5, and 1.0, were input into the model while the remaining parameters were retained as initialled. The hysteresis loops are shown in Fig. 5. This parameter had little influence on the overall hysteresis loops. Its key contribution was that it controlled the unloading stiffness and range of slippage. Larger values of γ increased the unloading stiffness and reduced the distance of the slipping.

Fig. 5. Hysteresis loops with different unloading degradation indices: (a) 0; (b) 0.3; (c) 0.5; (d) 1.0

Test Description

To investigate the coupling effect of shear load and tension load on CLT connections, experimental tests of angle bracket CLT connections and hold-down CLT connections under bi-axial loading were conducted. Due to space limitations and content relevance, the tests are described here concisely. The detailed setup, results, analyses, and discussions of the experiments can be found in (Liu and Lam 2016, 2018, 2019).

In the tested CLT connections, for the CLT panels, 5-layer panels made of graded No. 1/2 SPF lumber with a thickness of 169 mm were used. As shown in Fig. 6 (a), on each side of the angle bracket CLT connection, AE116 angle bracket was used with 8 Φ 4 x 60 nails, connected to the steel base by three M12 bolts. Two actuators were acting on the specimen, denoted as LC1 and LC2: LC 1 provided vertical load through a steel cable connected to the connection, while LC2 provided lateral load at the bottom of the connection. During each test, one load cell provided a constant load, while the other one provided a monotonic or cyclic load. The same setup was applied for hold-down connections as shown in Fig. 6 (b). On each side of the hold-down CLT connection, HTT5 hold-down was used with 12 Φ 4 x 60 nails, connected to the steel base by one M16 bolt.

Fig. 6. Schematic drawing of the experiment setup: (a) angle bracket test setup; (b) hold-down test setup

Fig. 7 (a) and Fig. 7 (b) present a representative test photo for angle bracket connection and hold-down connection, respectively.

Fig. 7. Representative test photos: (a) angle bracket test; (b) hold-down test

Four sets of connection tests were performed under bi-axial loading: 1) Set A: monotonic and cyclic shear loading with 4 levels of constant tension loads (0 kN, 20 kN, 30 kN, and 40 kN) on angle bracket connections; 2) Set B: monotonic and cyclic tension loading with 4 levels of constant shear loads (0 kN, 20 kN, 30 kN, and 40 kN) on angle bracket connections; 3) Set C: monotonic and cyclic shear loading with 5 levels of constant tension loads (0 kN, 20 kN, 30 kN, 40 kN, and 60 kN) on hold-down connections; 4) Set D: monotonic and cyclic tension loading with 3 levels of constant shear loads (0 kN, 10 kN, and 20 kN) on hold-down connections. All tests were conducted using a reverse cyclic protocol with predefined yield values which varied from configuration to configuration, depending on experimental yield values obtained from monotonic tests.

For each configuration, one monotonic and three/six cyclic tests were performed. In total, 88 tests were conducted: 22 tests for Set A, 22 tests for Set B, 26 tests for Set C, and 18 tests for Set D. The specimens were named under the following rules: the first two letters “AB” or “HD” denote “angle bracket connection” or “hold-down connection”; the following letter “S” or “T” denotes “constant shear load” or “constant tension load” in one direction; the following number denotes the constant load value; the letter after “T” and “S” representing the dynamic loading in the perpendicular direction; the following letter “C” or “M” denotes “cyclic loading” or “monotonic loading”; the number after “C” denotes the numbering of the specimen. For example, “HDS10TC2” represented the No. 2 hold-down specimen for cyclic tension loading with a co-existent shear load of 10 kN.

The force-displacement curves and the findings of the tests are presented in the next section comparing with modeling results.

CLT Connection Modeling

The CLT connections were simulated using pseudo-nail model with the optimized HYST algorithm. For each configuration, one representative specimen was modeled. In total, 32 pseudo-nail models were calibrated to cover all configurations. The models are validated versus the test results and the parameters are discussed in this section.

Model validation

The results from HYST model and test results are presented to demonstrate the efficacy of the optimized algorithm.

Fig. 8 presents the HYST model results versus test results of Set A, which are the angle bracket shear tests with a co-existent tension force. From those figures, first, it is noticed that the optimized HYST algorithm exhibited high consistence in modeling the monotonic behaviour of the connections in the four conditions. As shown from Fig. 8 (a) to Fig. 8 (d), with the introduction of co-existent tension force, the hysteresis behavior changed sharply. As the co-existent tension load increased, the shear performance of connectors was weakened, especially the strength, unloading stiffness, energy dissipation capacity and stability. The model showed satisfying adaptability in capturing those features. Comparing the curves in the red boxes in Fig. 8 (a) and Fig. 8 (b), the change of unloading was seized in this model, which is not able to achieve if using the modified HYST algorithm (Li and Lam 2015). In Fig. 8 (d), due to the instability of connections under high co-existent tension load, the modeling results had a certain difference to the test results in the last cycle as pointed by the arrows.

Fig. 8. HYST model versus test results of force-displacement curves in Set A: (a) 0 kN ; (b) 20 kN; (c) 30 kN; (d) 40 kN

Fig. 9 shows the comparisons of energy dissipation in cyclic tests for Set A. Good agreement can be observed, which also validated the accuracy of the optimized algorithm in modeling hysteresis behaviour.

Fig. 9. HYST model versus test results of energy dissipation in Set A: (a) 0 kN ; (b) 20 kN; (c) 30 kN; (d) 40 kN

The HYST model results versus test results of Set B, the hold-down shear tests with a co-existent tension force, are shown in Fig. 10. The results presented similar features as those of Set A. The change of unloading, highlighted in red boxes, and weakening of pinching effect, pointed by arrows, were even more visible in those five conditions comparing with Set A. The reloading stiffness degradation was more obvious, as shown in the circles in Fig.10 (a) and Fig. 10 (c). These features were captured by the model with high accuracy.

Fig. 10. HYST model versus test results of force-displacement curves in Set B: (a) 0 kN; (b) 20 kN; (c) 30 kN; (d) 40 kN; (e) 60 kN

The energy dissipated by the hysteresis loops using models indicated satisfying consistency with that of tests, as shown in Fig. 11.

Fig. 11. HYST model versus test results of energy dissipation in Set B: (a) 0 kN; (b) 20 kN; (c) 30 kN; (d) 40 kN; (e) 60 kN

For Set C, as shown in Fig. 12, the co-existent shear force weakened the axial loading capacity and energy dissipation capacity at large vertical displacements. The backbones deteriorated more severely than those in Set A and Set B for cyclic tension tests with co-existent tension force. At 40 kN co-existent shear force, the tension capacity dropped 25% compared to 0 kN co-existent shear force. This is simulated by changing the five parameters of equivalent wood embedment, Q_0, Q_1, Q_2, K_0, and $D_{\max}$, that influence the backbone of the pseudo-nail model. The setup of the tests, loading tension through a steel cable, limited the unloading and reloading. But the model still performed well in capturing the hysteresis loops with the real protocol recorded from cyclic tests.

Fig. 12. HYST model versus test results of energy dissipation in Set C: (a) 0 kN; (b) 20 kN; (c) 30 kN; (d) 40 kN

In Set D, the co-existent shear force weakened the energy dissipation capacity of hold-downs significantly at large vertical displacements, as shown in Fig. 13. The difference between model and test results in unloading is due to the relaxation of the loading cable. Otherwise, the accuracy of the model is sufficient compared to the test results.

Fig. 13. HYST model versus test results of force-displacement curves in Set D: (a) 0 kN; (b) 10 kN; (c) 20 kN

Based on above validations, it can be concluded that pseudo-nail model with the optimized HYST algorithm is a powerful finite-element based algorithm in simulating CLT connections under bi-axial loading, and more generally, nail-based wood connections under different loading protocols.

Parameter discussion

The parameters used to calculate the force-displacement curves are presented and discussed as below. One feature of the optimized algorithm is that it helps explain and understand the structural mechanisms of nail-based wood connections under complex loading.

In all models, the pseudo-nail had the same length (L) of 150 mm, diameter (D) of 8 mm, Elastic Modulus (E) of 200 GPa, and yielding strength (E_y) of 0.01 kN/mm^2. All angle bracket and hold-down connections were considered as stiff steel plate sheath with a thickness of 5 mm, and large embedment property parameters of Q_0 (100 kN/mm), Q_1 (100 kN/mm^2), Q_2 (200), K_0 (200 kN/mm^2), D_{max} (200 mm). α, β, and γ of the sheath had little influence on the performance.

The major differences between the models were the embedment property parameters of the equivalent wood embedment. Table 2 presents those parameters for each test configuration.

Table 2. Property parameters of equivalent wood embedment for each test configuration

For all monotonic tests, only the first five parameters Q_0, Q_1, Q_2, K_0, and D_{max} were needed in the models. For Set B and Set D, where tension cyclic tests were conducted, loading vertical force through a steel cable limited the accuracy of unloading and reloading. Thus the models also only adopted the first five parameters targeting the backbones. For the shear cyclic tests in Set A and Set D, the hysteresis behaviours of CLT connections were well captured. Subsequently, all 8 parameters played their roles in depicting the characteristics of CLT connections under bi-axial loading. In each set, the parameters of pure shear or tension tests were calibrated at first. After that, the rest tests with co-existent force were adjusted based on those parameters and at a principle of modifying the least number of parameters.

Since the parameters in nail shank and steel plate sheath are the same in all sets, the parameters of equivalent wood embedment are comparable. Furthermore, they provided explanation of the phenomenon in the tests in the sense of physics.

Co-existent forces weakened the loading and unloading in cyclic tests, which can be observed from the decreasing trend of the values of Q_0, Q_1, Q_2, K_0, and D_{max} in each set. The observation that CLT connections can hold strength after peak values longer for tension than shear was confirmed to the variations of parameter Q_2, 1.1 ~ 1.3 for shear, and 1.35 ~ 2.8 for tension. The fact that angle bracket has larger shear stiffness than hold-downs was reflected in the initial stiffness parameter K_0, 0.31 kN/mm^2 for angle bracket and 0.04 kN/mm^2 for hold-down. For hold-downs, the initial stiffness parameter K_0 was 0.04 kN/mm^2 for shear, and 4 kN/mm^2 for tension. This verified that hold-downs are stronger in tension than shear. The fact that CLT connections has more deformation capacities in shear of than tension was demonstrated through the parameter D_{max}, 35 mm ~ 50 mm for shear, and 7 mm ~ 11 mm for tension.

As for degradation parameters, the strength/reloading stiffness degradation factor α has been discussed in detail in Li *et al*. (2011). Larger value of α leads to severe strength degradation and reloading stiffness degradation. The unloading degradation needs two parameters to be captured. First, an exponential index γ was used to calculate the unloading stiffness value. The similar definition form as α guarantees the continuity and stability of the algorithm. Second, the algorithm needs to define an interval, in which the pseudo-nail is unloading with resistance. Thus, the gap size factor β is introduced and the interval is from βD_0 to D_0. Table 2 revealed that β become smaller under larger co-existent force. This is confirmed with the fact that larger co-existent force caused more resistance in the gap.

Fig. 14 is a representative curve showing the embedment properties of equivalent wood embedment of HDT30SC in the modified HYST algorithm generated from the parameters in Table 2.

Fig. 14. The embedment property curve for the equivalent wood embedment of HDT30S

The values of the curve are mostly contributed by Q_0 and Q_1, and weakly influenced by K_0, until D_{max} is reached. K_0 and Q_0 control its shape. Q_2 controls the shape of the right curve after D_{max}. The equivalent wood embedment provided resistance inside the gap from D_0 to $0.7D_0$. This gap size factor β and unloading stiffness index γ are the keys of capturing the coupling effect under bi-axial loading.

Model limitation

Despite the strong functionality of the optimized algorithm, it should be noted that under bi-axial loading, experimental results showed that for different co-existent force levels, the connections had different backbones, unloading and reloading paths. The optimized algorithm presents an intuitive way in explaining the mechanics of bi-axial loading, and has high accuracy in modeling different configurations. But it is an empirical model that needs to be calibrated using test data. If we want to use interpolation function method to generate an implementation model for dynamic analysis, we need more incremental co-existent force level tests. Besides, in the tests and modeling, bi-axial loading was conducted in a form of constant loading in one direction, and dynamic loading in the perpendicular direction. In the real structures, CLT connections are undertaking dynamic loads in both directions. The way of addressing the coupling effect of dynamic loads in both directions needs to be further studied.

Conclusions

In this paper, the expansion of an existing protocol-independent nail connection algorithm was presented and applied to simulate the coupling effect of CLT connections under bi-axial loading. The optimized HYST algorithm added unloading stiffness degradation feature to the original algorithms, which extends its sufficient application to nail-based timber connections that need to consider strength degradation, unloading/reloading stiffness degradation, pinching effect, and coupling effect. Using pseudo-nail model with this optimized HYST algorithm, four sets of CLT connection tests, Set A) monotonic/cyclic shear tests of angle bracket connections with four levels of co-existent tension force, Set B) monotonic/cyclic shear tests of hold-down connections with five levels of co-existent tension force, Set C) monotonic/cyclic tension tests of angle bracket connections with four levels of co-existent shear force, and Set D) monotonic/cyclic tension tests of hold-down connections with three levels of co-existent shear force, were modeled. The simulation provided a mechanism-based way and physical explanation to understand the behaviour of CLT connections under bi-axial loading protocols.

The model results were compared with test results for all 32 configurations by hysteresis loops and energy dissipations, which indicated strong accuracy and efficiency of the pseudo-nail modeling method and the optimized HYST algorithm. The newly observed unloading stiffness degradation phenomenon in CLT connections, which is caused by co-existence force, was captured by the two introduced parameters in equivalent wood embedment properties, gap size factor β and unloading stiffness degradation index γ. Based on the simulation results, the parameters of the optimized HYST algorithm were discussed to explain the mechanisms of the structural behaviour of CLT connections. The observations in the tests were identical with the variations of model parameters. The key feature of coupling effect of bi-axial loading, that nails undertake loads in the gap in wood embedment, was explained and quantified by the gap size factor β and unloading stiffness degradation index γ. Both the gap size factor β and unloading stiffness degradation index γ have individual mechanical meanings. Gap size factor presents the interval in the gap where pseudo-nail receives resistance due to co-existent load. Unloading stiffness degradation index accounts for the stiffness degradation in this interval. The optimized model extended the application scope of HYST and strongly improved its accuracy in dynamic analysis.

As for this research, the modeling of bi-axial loading effect of CLT connections with constant load in one direction and dynamic load in the perpendicular direction has reached the goals. Still, further research on dynamic bi-axial loading of CLT connections is required.

References

Ceccotti, A. (2008). "New technologies for construction of medium-rise buildings in seismic regions: the XLAM case." Struct.Eng.Int., 18(2), 156-165.

Ceccotti, A., and Follesa, M. (2006). "Seismic behaviour of multi-storey X-lam buildings." Proc. International Workshop on" Earthquake Engineering on Timber Structures" Coimbra, Portugal.

Ceccotti, A., Sandhaas, C., Okabe, M., Yasumura, M., Minowa, C., and Kawai, N. (2013). "SOFIE project–3D shaking table test on a seven- storey full- scale cross- laminated timber building." Earthquake Eng.Struct.Dyn., 42(13), 2003-2021.

Dujic, B., and Zarnic, R. (2005). "Report on evaluation of racking strength of KLH system." University of Ljubljana, Faculty of Civil and Geodetical Engineering, Slovenia.

Dujic, B., Aicher, S., and Zarnic, R. (2006). "Testing of wooden wall panels applying realistic boundary conditions." Proceedings of the 9th World Conference on Timber Engineering, Portland, Oregon, USA.

Dujic, B., Klobcar, S., and Zarnic, R. (2008). "Shear capacity of cross-laminated wooden walls." Proceedings of the 10th World Conference on Timber Engineering, Miyazaki, Japan.

Folz, B., and Filiatrault, A. (2001). "Cyclic analysis of wood shear walls." J.Struct.Eng., 127(4), 433-441.

Foschi, R. O., Yao, F., and Rogerson, D. (2000). "Determining embedment response parameters from connector tests." World Conference on Timber engineering, Whistler, BC, Canada.

Fragiacomo, M., Dujic, B., and Sustersic, I. (2011). "Elastic and ductile design of multi-storey crosslam massive wooden buildings under seismic actions." Eng.Struct., 33(11), 3043-3053.

Ganey, R. S. (2015). "Seismic design and testing of rocking cross laminated timber walls". University of Washington, US.

Gavric, I., Ceccotti, I., and Fragiacomo, M. (2011). Experimental cyclic tests on cross-laminated timber panels and typical connections. Holz. bau Forschungs Gmbh.

Gu, J., and Lam, F. (2004). "Simplified mechanics-based wood frame shear wall model." Proc., 13th World Conf. on Earthquake Engineering, Vancouver Canada.

Li, M., Foschi, R. O., and Lam, F. (2011). "Modeling hysteretic behavior of wood shear walls with a protocol-independent nail connection algorithm." J.Struct.Eng., 138(1), 99-108.

Li, M., and Lam, F. (2009). "Lateral performance of nonsymmetric diagonal-braced wood shear walls." J.Struct.Eng., 135(2), 178-186.

Li, M., Lam, F., and Foschi, R. O. (2009). "Seismic reliability analysis of diagonal-braced and structural-panel-sheathed wood shear walls." J.Struct.Eng., 135(5), 587-596.

Li, M., Foschi, R. O., and Lam, F. (2011). "Modeling hysteretic behavior of wood shear walls with a protocol-independent nail connection algorithm." Journal of Structural Engineering, 138(1), 99-108.

Li, M., and Lam, F. (2015). "Lateral behaviour of cross laminated timber shear walls under reversed cyclic loads." Proc., 10th Pacific Conf. on Earthquake Engineering, Seismology Research Centre, VIC, Australia.

Li, Z., He, M., Lam, F., Li, M., Ma, R., and Ma, Z. (2014). "Finite element modeling and parametric analysis of timber–steel hybrid structures." The Structural Design of Tall and Special Buildings, 23(14), 1045-1063.

Lim, H., Lam, F., Foschi, R. O., and Li, M. (2017). "Modeling Load-Displacement Hysteresis Relationship of a Single-Shear Nail Connection." J.Eng.Mech., 143(6), 04017015.

Liu, J., and Lam, F. (2014). "Numerical simulation for the seismic behaviour of mid-rise CLT shear walls with coupling beams." 13th World Conference on Timber Engineering (WCTE 2014), Quebec City, Canada.

Liu, J., and Lam, F. (2016). "Experimental test of cross laminated timber connections under bi-directional loading." 2016 World Conference on Timber Engineering, WCTE 2016, University of Vienna, Austria.

Liu, J., and Lam, F. (2018). "Experimental test of coupling effect on CLT angle bracket connections." Eng.Struct., 171 862-873.

Liu, J., and Lam, F. (2019). "Experimental test of coupling effect on CLT hold-down connections." Eng.Struct., 178 586-602.

Lowes, L. N., Mitra, N., and Altoontash, A. (2003). "A beam-column joint model for simulating the earthquake response of reinforced concrete frames." University of California, Berkeley, US.

Mahdavifar, V., Sinha, A., Barbosa, A. R., Muszynski, L., and Gupta, R. (2018). "Lateral and withdrawal capacity of fasteners on hybrid cross-laminated timber panels." Journal of Materials in Civil Engineering, 30(9), 04018226.

Mahdavifar, V., Barbosa, A. R., Sinha, A., Muszynski, L., Gupta, R., and Pryor, S. E. (2018). "Hysteretic response of metal connections on hybrid Cross-Laminated Timber panels." Journal of Structural Engineering, 145(1), 04018237.

Pei, S., Popovski, M., and van de Lindt, John W. (2013). "Analytical study on seismic force modification factors for cross-laminated timber buildings." Canadian Journal of Civil Engineering, 40(9), 887-896.

Pei, S., Van De Lindt, J W, Popovski, M., Berman, J. W., Dolan, J. D., Ricles, J., Sause, R., Blomgren, H., and Rammer, D. R. (2014). "Cross-laminated timber for seismic regions: Progress and challenges for research and implementation." J.Struct.Eng., 142(4), E2514001.

Pei, S., Rammer, D., Popovski, M., Williamson, T., Line, P., and van de Lindt, John W. (2016). "An Overview of CLT Research and Implementation in North America." 2016 World Conference on Timber Engineering, WCTE 2016, University of Vienna, Austria.

Popovski, M., Schneider, J., and Schweinsteiger, M. (2010). "Lateral load resistance of cross-laminated wood panels." In Proceedings of 11th World Conference on Timber Engineering, Riva del Garda, Trentino, Italy.

Popovski, M., and Gavric, I. (2015). "Performance of a 2-story CLT house subjected to lateral loads." J.Struct.Eng., 142(4), E4015006.

Pozza, L., Scotta, R., and Vitaliani, R. (2009). "A non linear numerical model for the assessment of the seismic behaviour and ductility factor of X-lam timber structures." Proceeding of international Symposium on Timber Structures, Istanbul, Turkey.

Pozza, L., Saetta, A., Savoia, M., and Talledo, D. (2017). "Coupled axial-shear numerical model for CLT connections." Construction and Building Materials, 150 568-582.

Rinaldin, G., Amadio, C., and Fragiacomo, M. (2013). "A component approach for the hysteretic behaviour of connections in cross- laminated wooden structures." Earthquake Eng.Struct.Dyn., 42(13), 2023-2042.

Schneider, J., Karacabeyli, E., Popovski, M., Stiemer, S. F., and Tesfamariam, S. (2013). "Damage assessment of connections used in cross-laminated timber subject to cyclic loads." J.Perform.Constr.Facil., 28(6), A4014008.

Shen, Y., Schneider, J., Tesfamariam, S., Stiemer, S. F., and Mu, Z. (2013). "Hysteresis behavior of bracket connection in cross-laminated-timber shear walls." Constr.Build.Mater., 48 980-991.

Tomasi, R., and Smith, I. (2014). "Experimental characterization of monotonic and cyclic loading responses of CLT panel-to-foundation angle bracket connections." J.Mater.Civ.Eng., 27(6), 04014189.

van de Lindt, J. W., Furley, J., Amini, M. O., Pei, S., Tamagnone, G., Barbosa, A. R., Rammer, D., Line, P., Fragiacomoi, M., and Popovski, M. (2019). "Experimental seismic behavior of a two-story CLT platform building. " Eng.Struct., 183, 408-422.

Zhang, X., Fairhurst, M., and Tannert, T. (2015). "Ductility estimation for a novel timber–steel hybrid system." J.Struct.Eng., 142(4), E4015001.

Acknowledgement

The support from Timber Engineering and Applied Mechanics (TEAM) laboratory at University of British Columbia (UBC) is acknowledged. The project is funded by NSERC Strategic Network on Innovative Wood Products and Building Systems (NEWBuildS).

Tables:

Table 1. Descriptions of embedment property parameters in optimized HYST algorithm

Parameter	Description
K_0	Initial stiffness
Q_0	Intercept of the asymptote at the maximum compressive response
Q_1	Slope of the asymptote at the maximum compressive response
Q_2	Post-peak decay factor
D_{max}	Displacement at the maximum compressive response
α	Strength and reloading degradation index
β	Gap size factor
γ	Unloading degradation index

Table 2. Property parameters of equivalent wood embedment for each test configuration

Set	Configuration	Q_0 (kN/mm)	Q_1 (kN/mm^2)	Q_2	K_0 (kN/mm^2)	D_{max} (mm)	α	β	γ
A	ABT0SM	0.16	0.22	1.2	0.31	32	-	-	-
	ABT0SC	0.16	0.20	1.3	0.31	35	0.15	1	0.2
	ABT20SM	0.16	0.18	1.1	0.31	39	-	-	-
	ABT20SC	0.16	0.16	1.3	0.31	35	0.2	0.3	0.7
	ABT30SM	0.16	0.18	1.1	0.31	35	-	-	-
	ABT30SC	0.16	0.16	1.3	0.31	35	0.2	0.2	0.7
	ABT40SM	0.16	0.16	1.1	0.31	35	-	-	-
	ABT40SC	0.16	0.16	1.3	0.16	35	0.2	0.1	1
B	ABS0TM	4	0.5	1.35	2	11	-	-	-
	ABS0TC	4	0.3	1.35	2	10	-	-	-
	ABS20TM	4	0.5	1.35	3	11	-	-	-
	ABS20TC	4	0.28	1.8	2	10	-	-	-
	ABS30TM	4	0.5	1.35	1	9	-	-	-
	ABS30TC	4	0.3	2	1.5	7	-	-	-
	ABS40TM	4	0.5	1.35	1	7.5	-	-	-
	ABS40TC	4	0.2	1.2	4	8	-	-	-
C	HDT0SM	0.26	0.025	1.2	0.04	45	-	-	-
	HDT0SC	0.26	0.02	1.2	0.1	45	0.15	1	0
	HDT20SM	0.26	0.028	1.2	0.05	50	-	-	-
	HDT20SC	0.26	0.015	1.2	0.05	45	0.4	0.8	0.8
	HDT30SM	0.26	0.03	1.2	0.04	50	-	-	-
	HDT30SC	0.26	0.015	1.2	0.05	45	0.5	0.7	0.9
	HDT40SM	0.26	0.03	1.2	0.04	50	-	-	-
	HDT40SC	0.26	0.024	1.2	0.05	45	0.5	0.3	0.5
	HDT60SM	0.26	0.033	1.2	0.04	50	-	-	-
	HDT60SC	0.26	0.024	1.2	0.05	45	0.5	0.1	0.5
D	HDS0TM	7.5	0.15	2.3	5	8	-	-	-
	HDS0TC	8	0.15	2.3	4.5	10	-	-	-
	HDS10TM	7.5	0.15	1.3	4	10	-	-	-
	HDS10TC	8	0.12	2	4	7	-	-	-
	HDS20TM	7.5	0.15	1.3	4	10	-	-	-
	HDS20TC	7	0.1	2.8	4	10	-	-	-

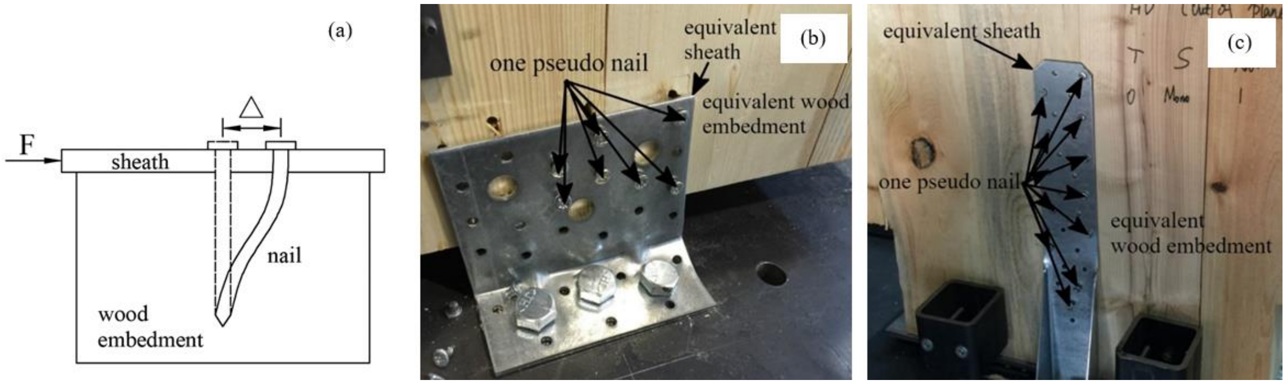

Fig. 1. (a) nail connector model; (b) pseudo-nail model of angle bracket connection; (c) pseudo-nail model of hold-down connection

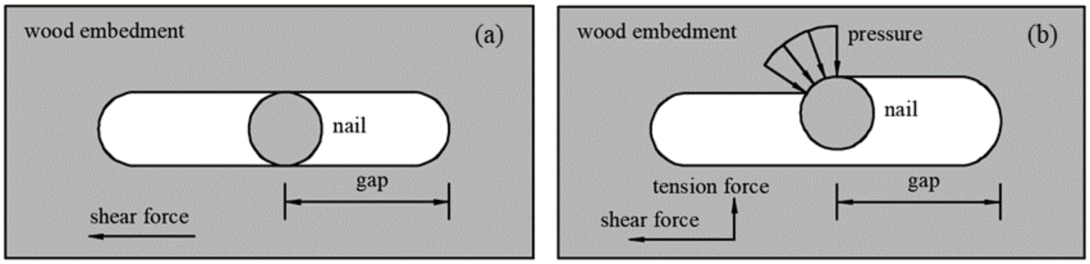

Fig. 2. Schematic section views of nails in the wood embedment: (a) nail movement under shear force with no co-existent tension load; (b) nail movement under shear force with co-existent tension load

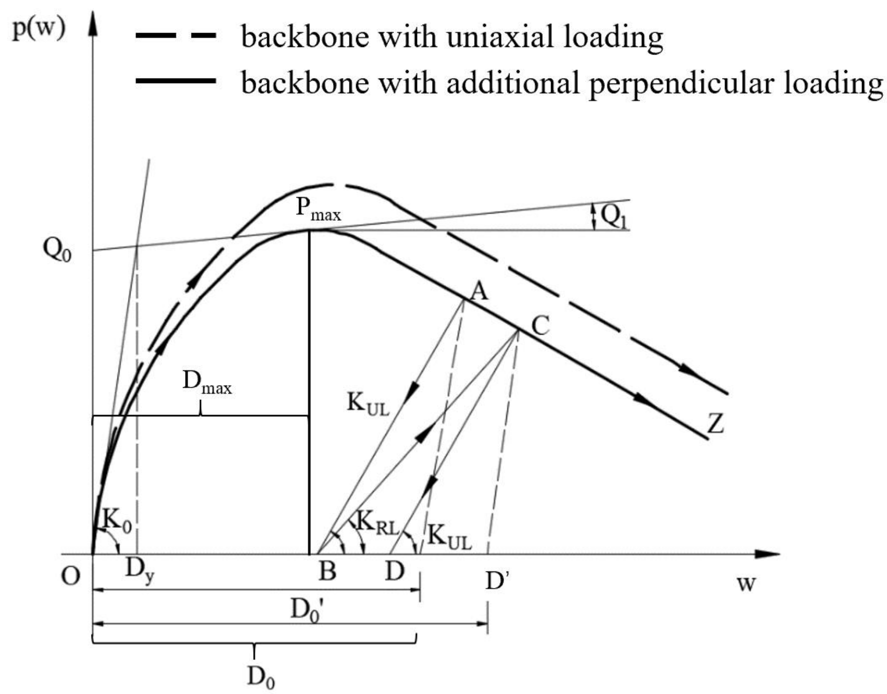

Fig. 3. Embedment properties in the optimized HYST algorithm

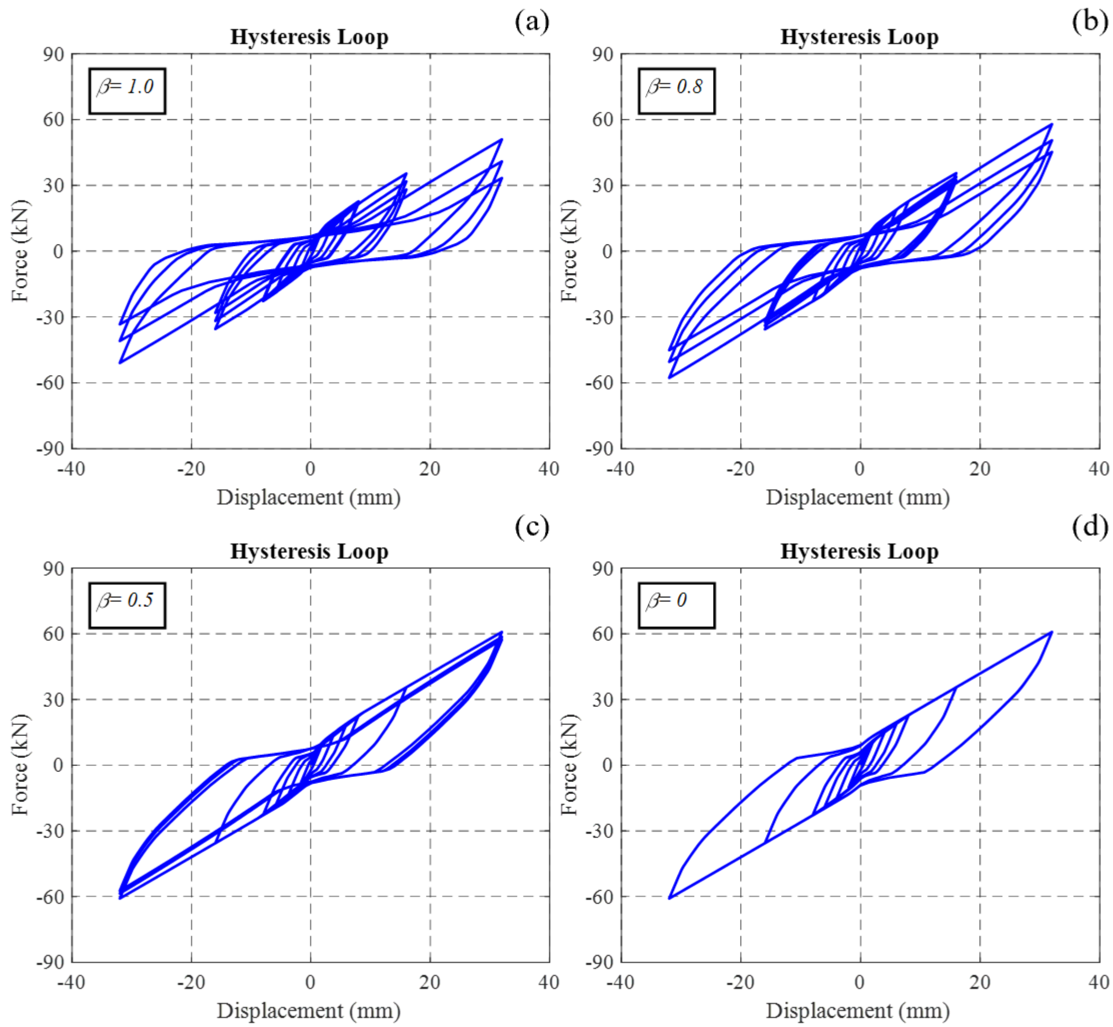

Fig. 4. Hysteresis loops with different gap size factors: (a) 1.0; (b) 0.8; (c) 0.5; (d) 0

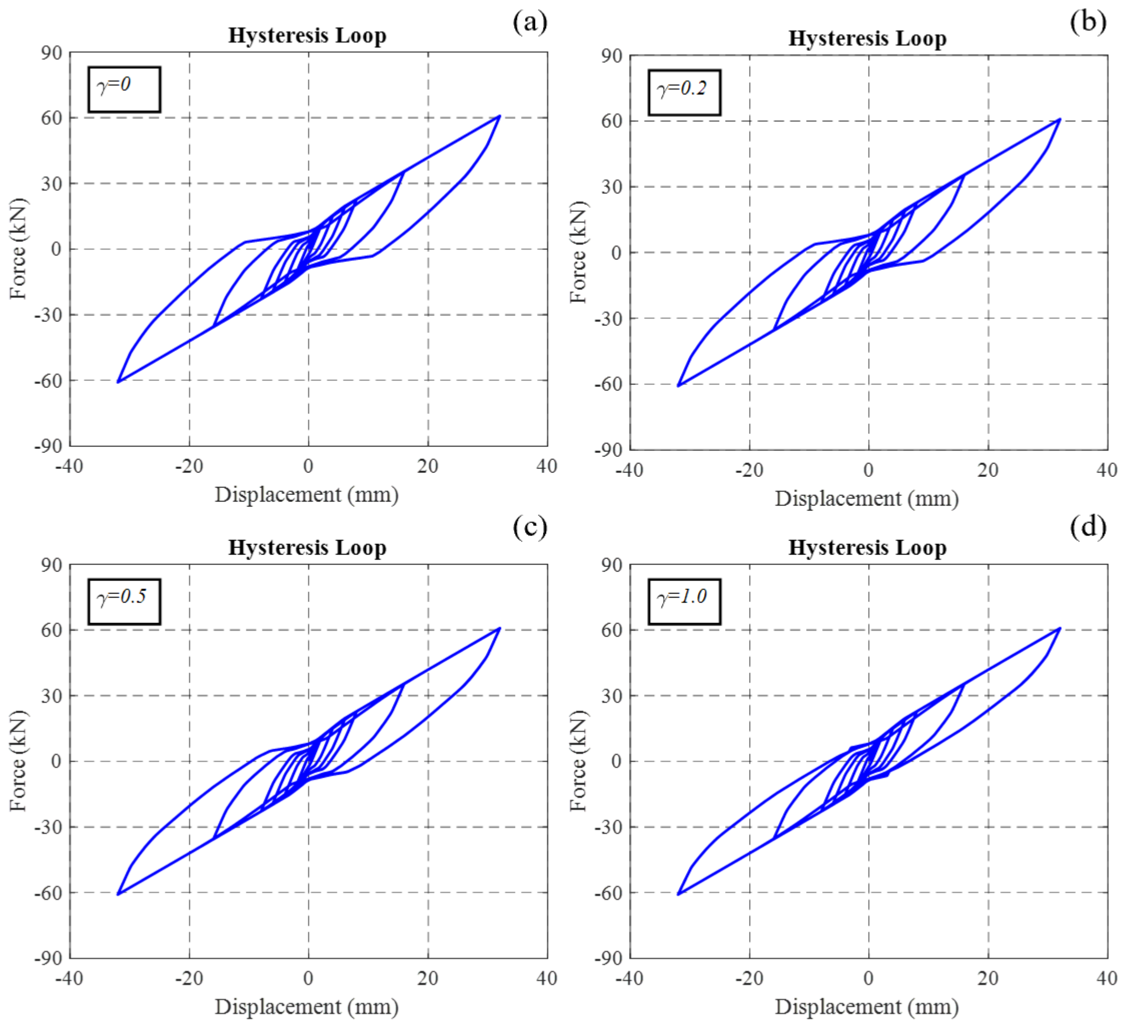

Fig. 5. Hysteresis loops with different unloading degradation indices: (a) 0; (b) 0.3; (c) 0.5; (d) 1.0

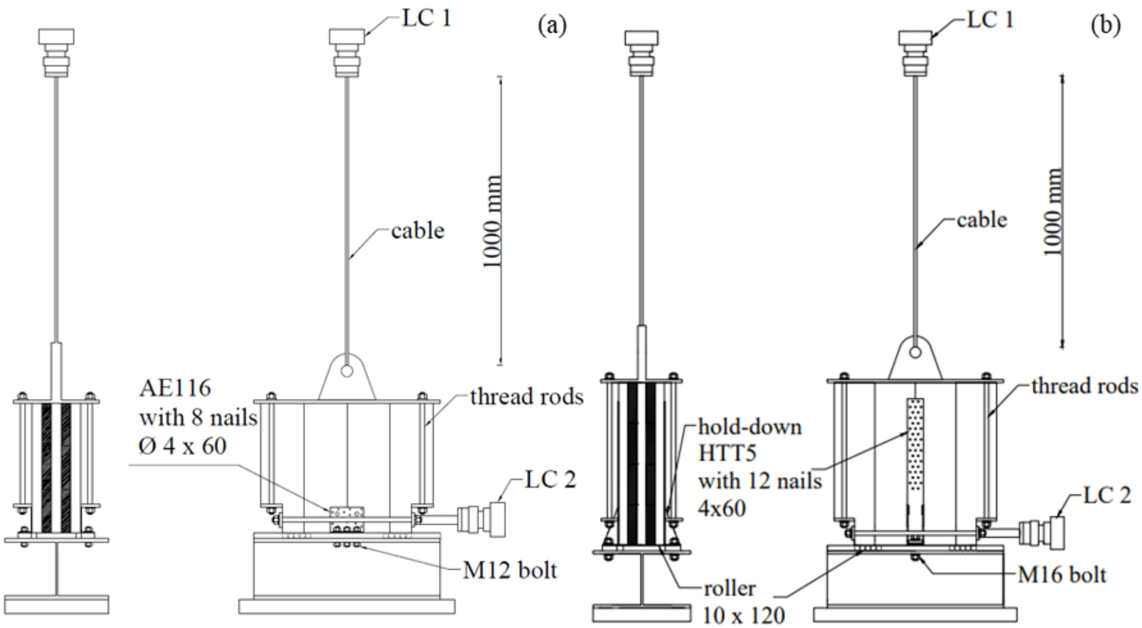

Fig. 6. Schematic drawing of the experiment setup: (a) angle bracket test setup; (b) hold-down test setup

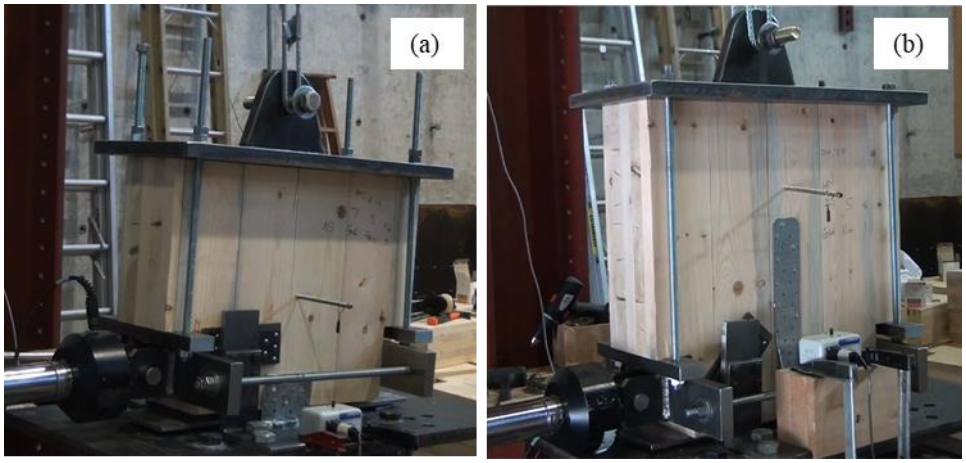

Fig. 7. Representative test photos: (a) angle bracket test; (b) hold-down test

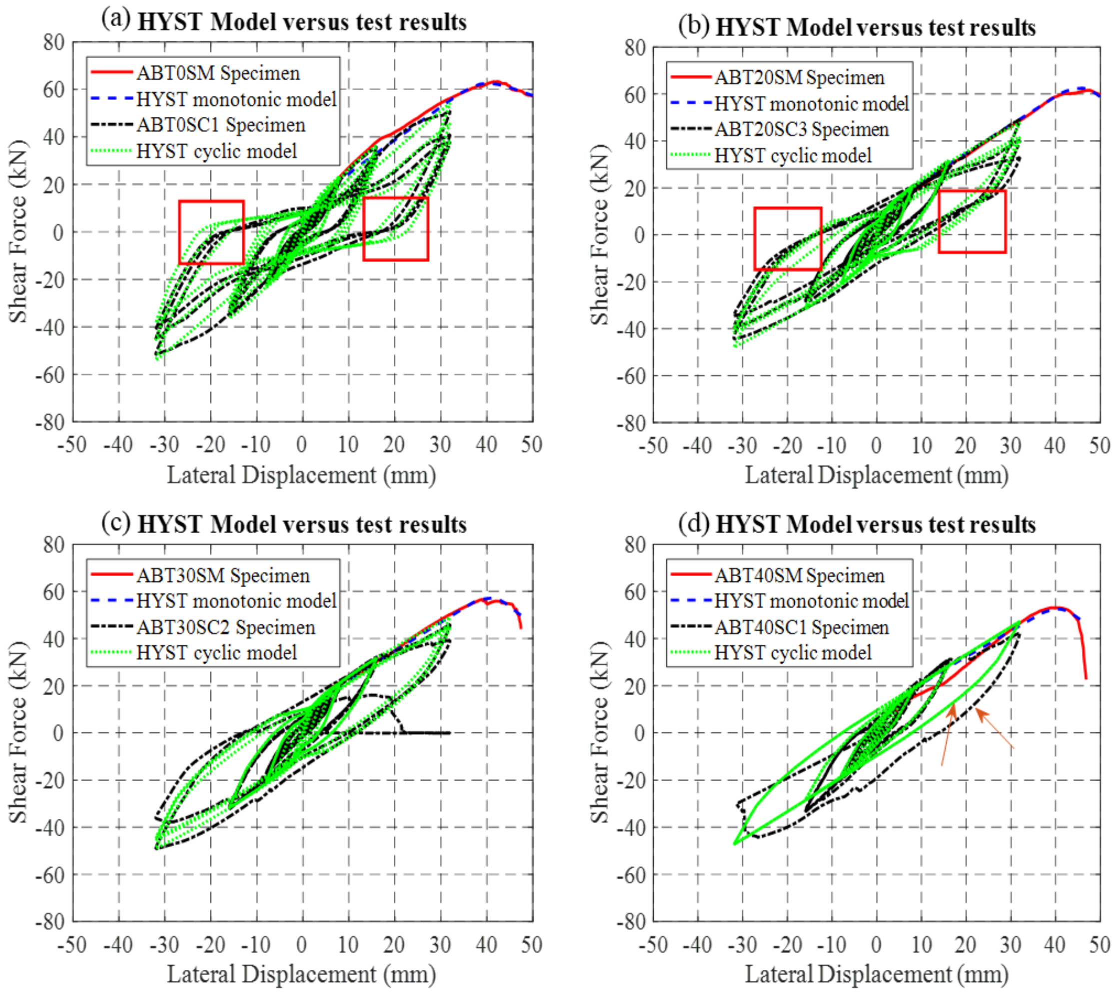

Fig. 8. HYST model versus test results of force-displacement curves in Set A: (a) 0 kN ; (b) 20 kN; (c) 30 kN; (d) 40 kN

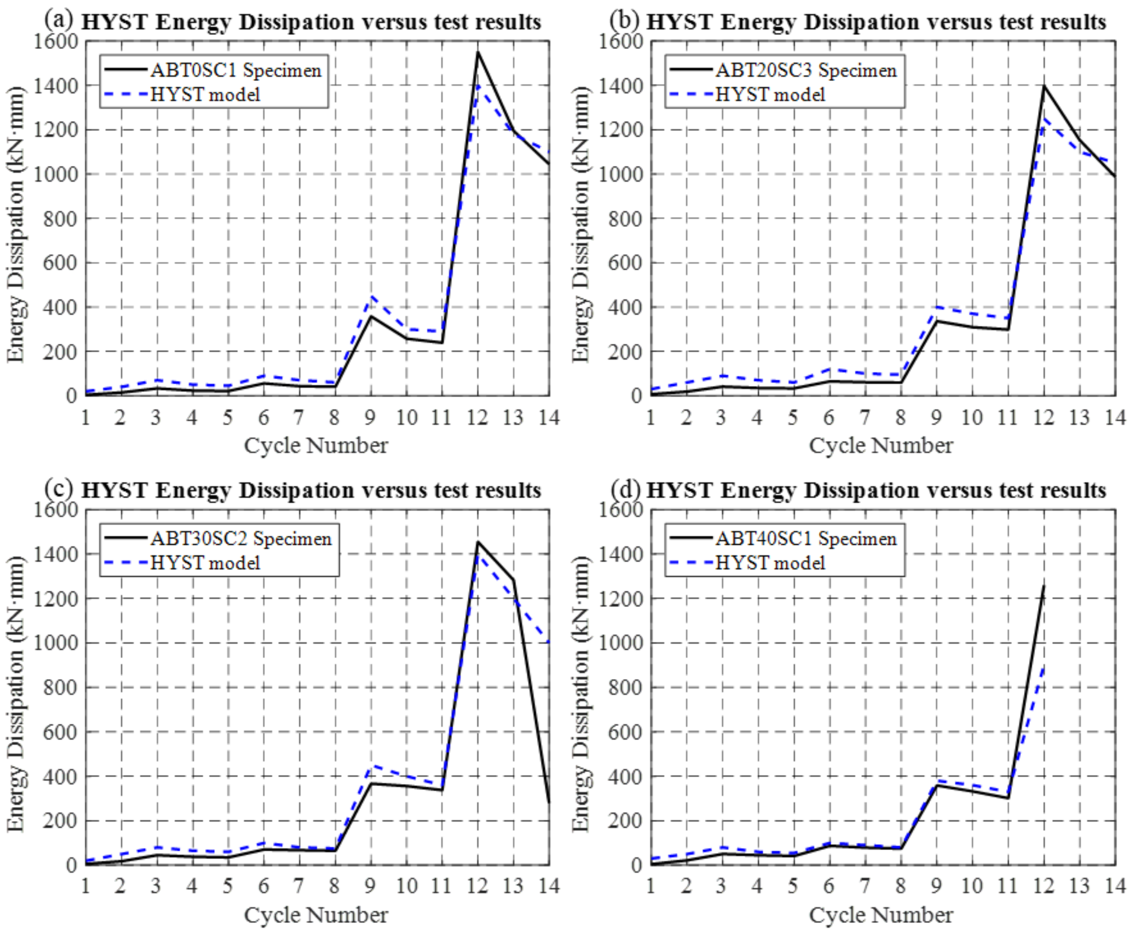

Fig. 9. HYST model versus test results of energy dissipation in Set A: (a) 0 kN ; (b) 20 kN; (c) 30 kN; (d) 40 kN

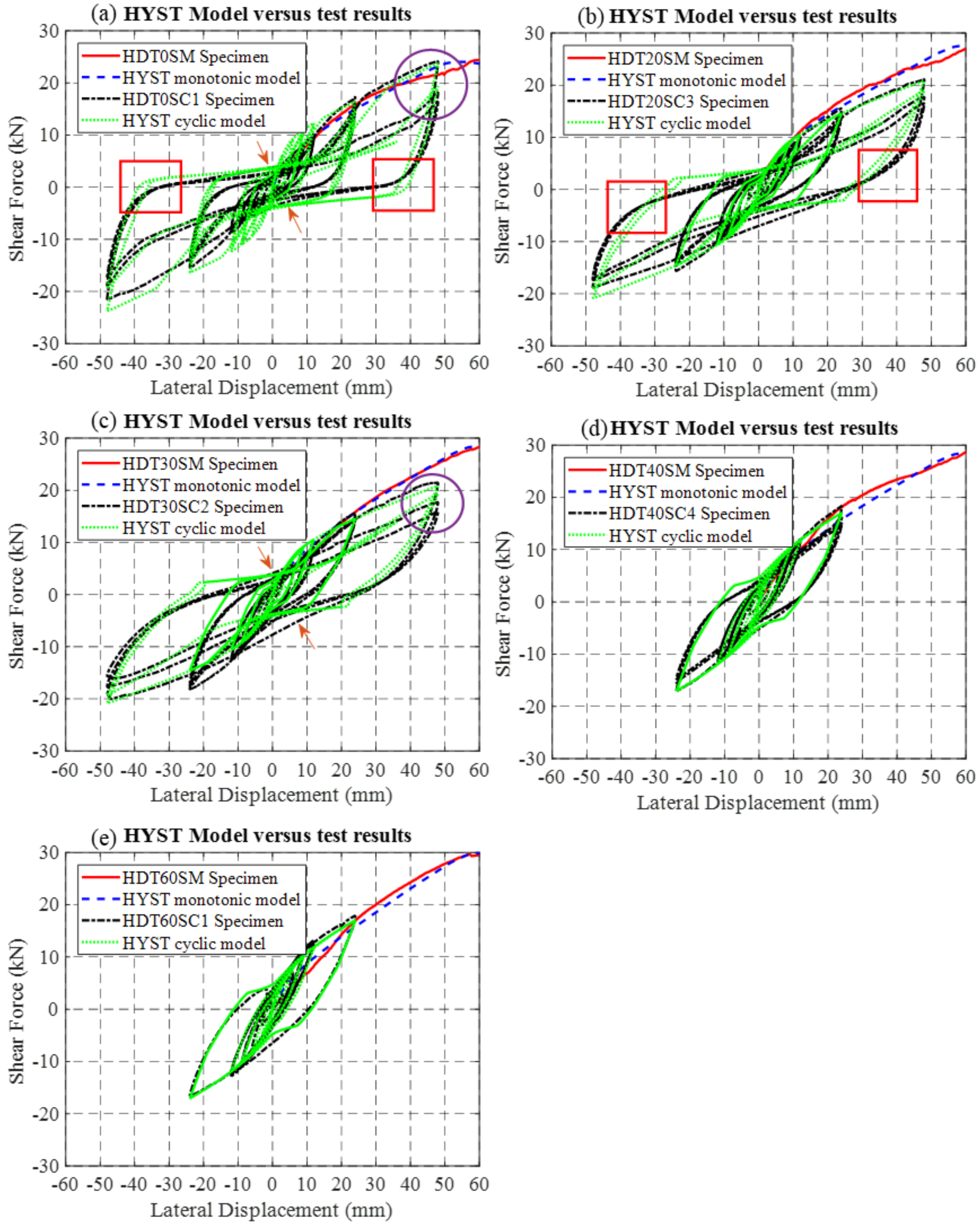

Fig. 10. HYST model versus test results of force-displacement curves in Set B: (a) 0 kN; (b) 20 kN; (c) 30 kN; (d) 40 kN; (e) 60 kN

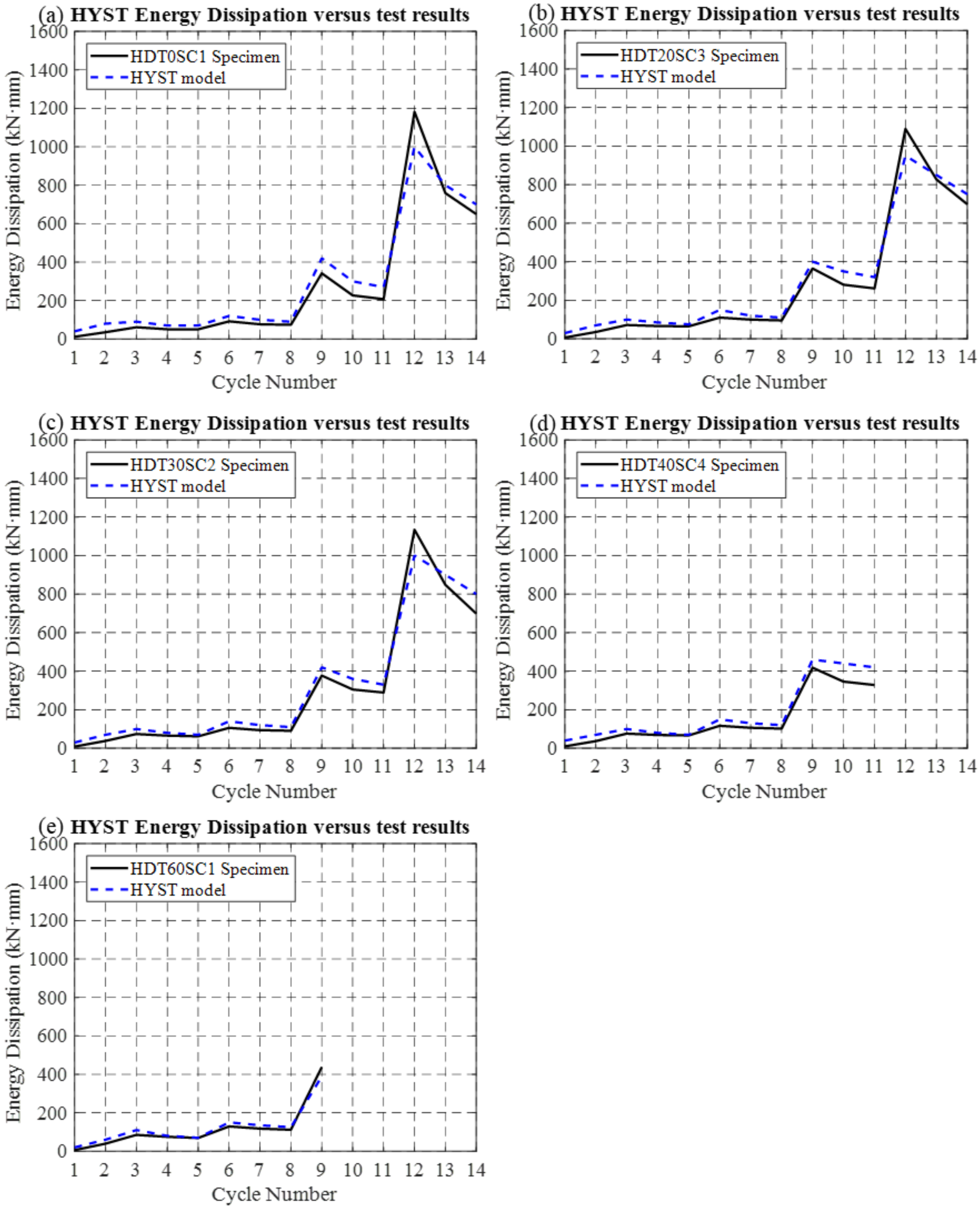

Fig. 11. HYST model versus test results of energy dissipation in Set B: (a) 0 kN; (b) 20 kN; (c) 30 kN; (d) 40 kN; (e) 60 kN

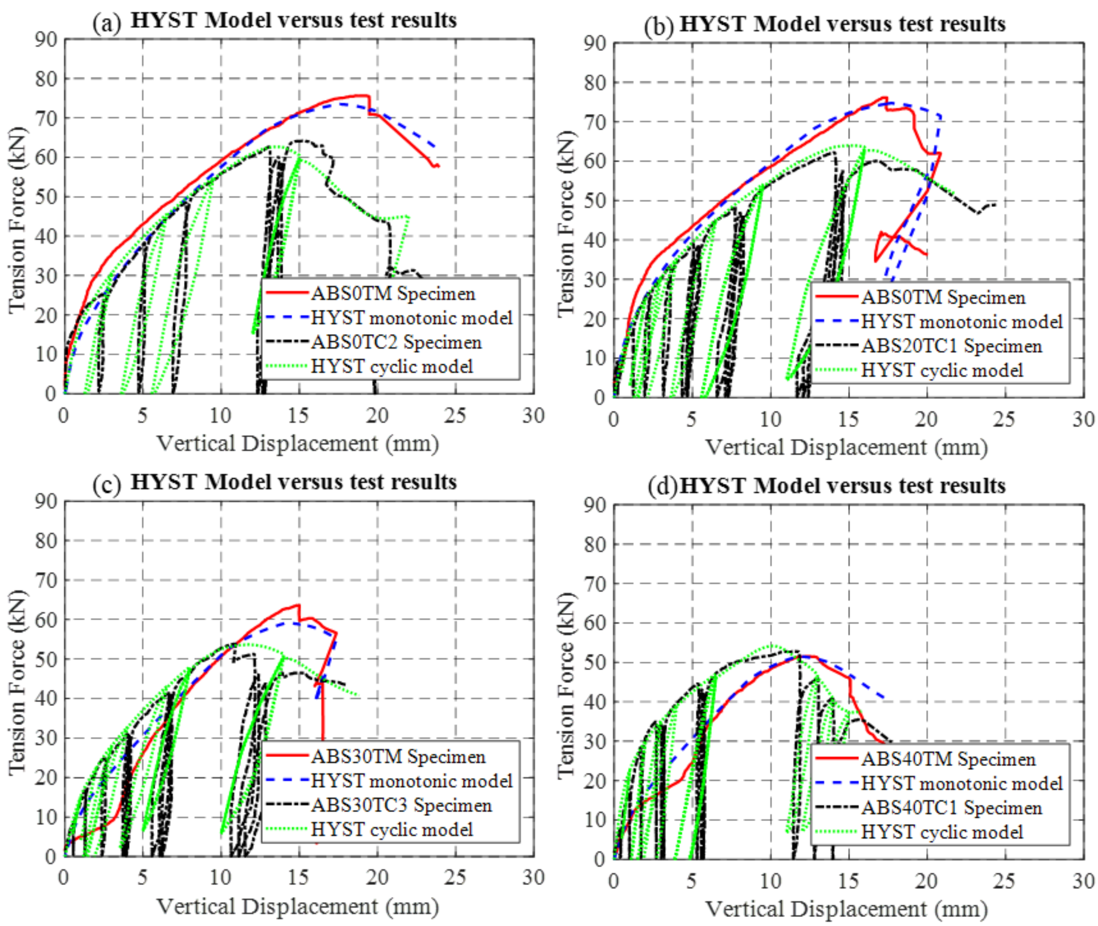

Fig. 12. HYST model versus test results of energy dissipation in Set C: (a) 0 kN; (b) 20 kN; (c) 30 kN; (d) 40 kN

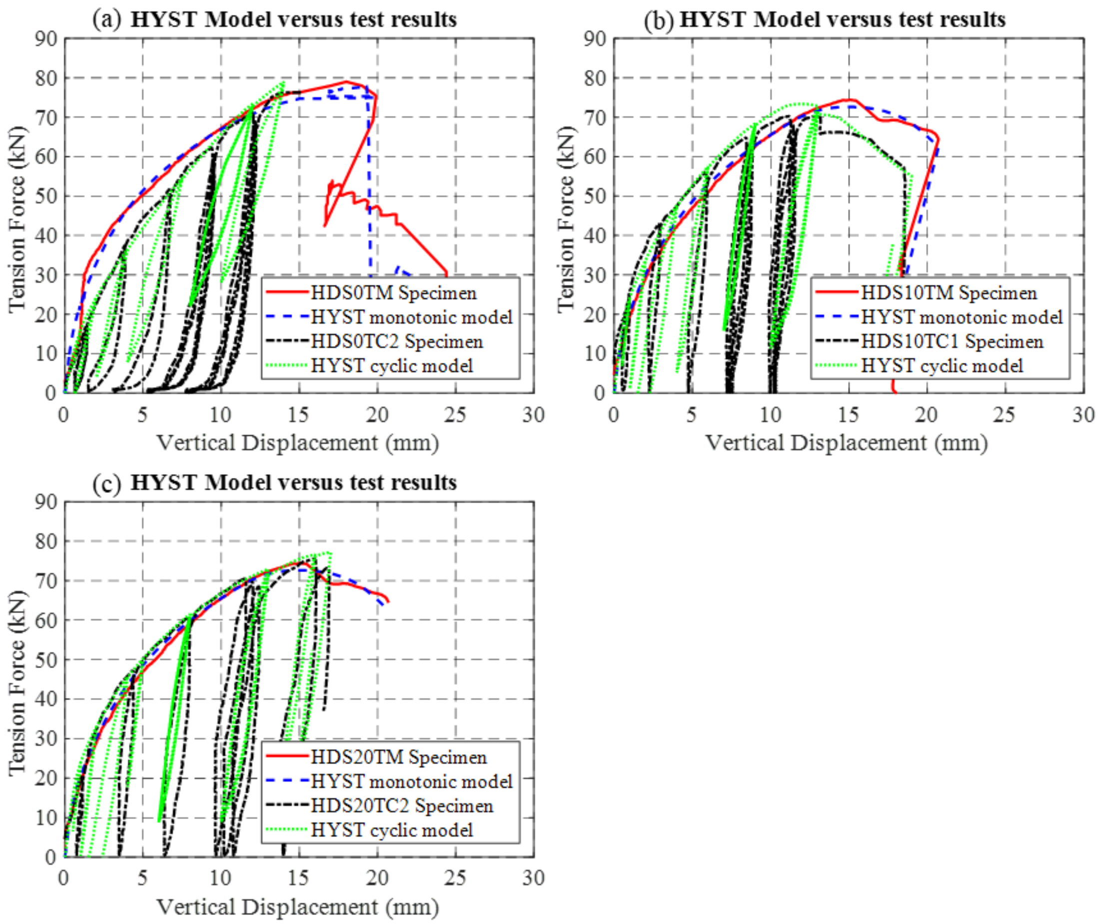

Fig. 13. HYST model versus test results of force-displacement curves in Set D: (a) 0 kN; (b) 10 kN; (c) 20 kN

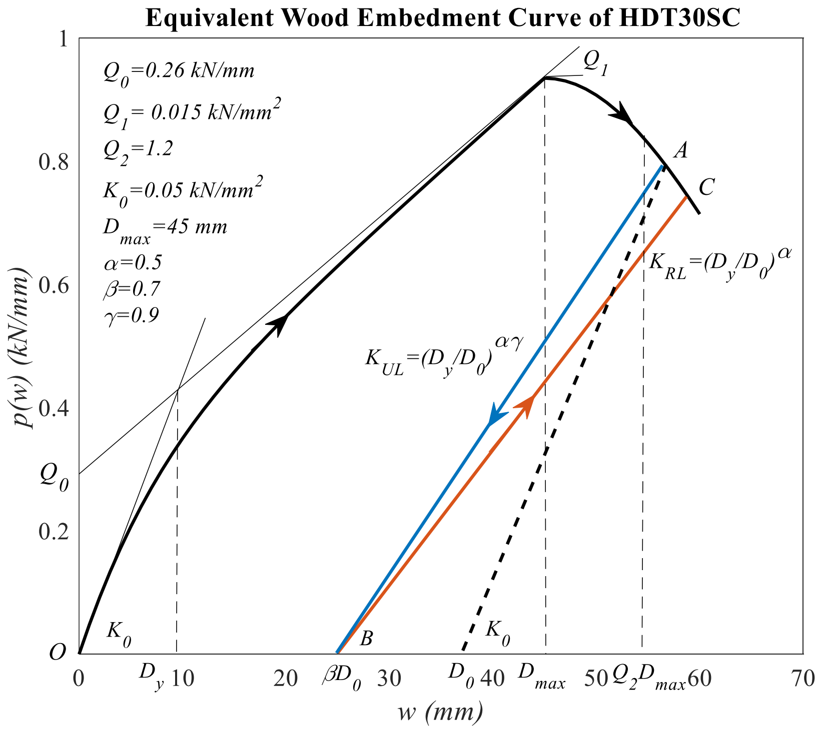

Fig. 14. The embedment property curve for the equivalent wood embedment of HDT30S

Fig. 1. (a) nail connector model; (b) pseudo-nail model of angle bracket connection; (c) pseudo-nail model of hold-down connection

Fig. 2. Schematic section views of nails in the wood embedment: (a) nail movement under shear force with no co-existent tension load; (b) nail movement under shear force with co-existent tension load

Fig. 3. Embedment properties in the optimized HYST algorithm

Fig. 4. Hysteresis loops with different gap size factors: (a) 1.0; (b) 0.8; (c) 0.5; (d) 0

Fig. 5. Hysteresis loops with different unloading degradation indices: (a) 0; (b) 0.3; (c) 0.5; (d) 1.0

Fig. 6. Schematic drawing of the experiment setup: (a) angle bracket test setup; (b) hold-down test setup

Fig. 7. Representative test photos: (a) angle bracket test; (b) hold-down test

Fig. 8. HYST model versus test results of force-displacement curves in Set A: (a) 0 kN ; (b) 20 kN; (c) 30 kN; (d) 40 kN

Fig. 9. HYST model versus test results of energy dissipation in Set A: (a) 0 kN ; (b) 20 kN; (c) 30 kN; (d) 40 kN

Fig. 10. HYST model versus test results of force-displacement curves in Set B: (a) 0 kN; (b) 20 kN; (c) 30 kN; (d) 40 kN; (e) 60 kN

Fig. 11. HYST model versus test results of energy dissipation in Set B: (a) 0 kN; (b) 20 kN; (c) 30 kN; (d) 40 kN; (e) 60 kN

Fig. 12. HYST model versus test results of energy dissipation in Set C: (a) 0 kN; (b) 20 kN; (c) 30 kN; (d) 40 kN

Fig. 13. HYST model versus test results of force-displacement curves in Set D: (a) 0 kN; (b) 10 kN; (c) 20 kN

Fig. 14. The embedment property curve for the equivalent wood embedment of HDT30S

ASCE Authorship, Originality, and Copyright Transfer Agreement

Publication Title: Journal of Structural Engineering

Manuscript Title/Number: Modeling the Coupling Effect of CLT Connections under Bi-axial Loading

Author(s) – **Names, postal addresses, and e-mail addresses of all authors**

Jingjing Liu,2842-2424 Main Mall, BC, Vancouver,Canada, jingjing.liu@alumni.ubc.ca; Frank Lam,2424 Main Mall,BC, Vancouver,Canada, frank.lam@ubc.ca; Ricardo O. Foschi, 6250 Applied Science Lane, BC, V6T1Z4, Vancouver, Canada, rfoschi@shaw.ca; Minghao Li,69 Creyke Road, Christchurch, New Zealand, minghao.li@canterbury.ac.nz

I. Authorship Responsibility

To protect the integrity of authorship, only people who have significantly contributed to the research or project and manuscript preparation shall be listed as coauthors. The corresponding author attests to the fact that anyone named as a coauthor has seen the final version of the manuscript and has agreed to its submission for publication. Deceased persons who meet the criteria for coauthorship shall be included, with a footnote reporting date of death. No fictitious name shall be given as an author or coauthor. An author who submits a manuscript for publication accepts responsibility for having properly included all, and only, qualified coauthors.

II. Originality of Content

ASCE respects the copyright ownership of other publishers. ASCE requires authors to obtain permission from the copyright holder to reproduce any material that (1) they did not create themselves and/or (2) has been previously published, to include the authors' own work for which copyright was transferred to an entity other than ASCE. For any figures, tables, or text blocks exceeding 100 words from a journal article or 500 words from a book, written permission from the copyright holder must be obtained and supplied with the submission. Each author has a responsibility to identify materials that require permission by including a citation in the figure or table caption or in extracted text.

More information can be found in the guide "Publishing in ASCE Journals: Manuscript Submission and Revision Requirements" (http://ascelibrary.org/doi/pdf/10.1061/9780784479018.ch05). Regardless of acceptance, no manuscript or part of a manuscript will be published by ASCE without proper verification of all necessary permissions to re-use. ASCE accepts no responsibility for verifying permissions provided by the author. Any breach of copyright will result in retraction of the published manuscript.

III. Copyright Transfer

ASCE requires that authors or their agents assign copyright to ASCE for all original content published by ASCE. The author(s) warrant(s) that the above-cited manuscript is the original work of the author(s) and has never been published in its present form.

The undersigned, with the consent of all authors, hereby transfers, to the extent that there is copyright to be transferred, the exclusive copyright interest in the above-cited manuscript (subsequently called the "work") in this and all subsequent editions of the work (to include closures and errata), and in derivatives, translations, or ancillaries, in English and in foreign translations, in all formats and media of expression now known or later developed, including electronic, to the American Society of Civil Engineers subject to the following:

- The undersigned author and all coauthors retain the right to revise, adapt, prepare derivative works, present orally, or distribute the work, provided that all such use is for the personal noncommercial benefit of the author(s) and is consistent with any prior contractual agreement between the undersigned and/or coauthors and their employer(s).
- No proprietary right other than copyright is claimed by ASCE.
- This agreement will be rendered null and void if (1) the manuscript is not accepted for publication by ASCE, (2) is withdrawn by the author prior to publication (online or in print), (3) ASCE Open Access is purchased by the author.
- Authors may post a PDF of the ASCE-published version of their work on their employers' ***Intranet*** with password protection. The following statement must appear with the work: "This material may be downloaded for personal use only. Any other use requires prior permission of the American Society of Civil Engineers."
- Authors may post the ***final draft*** of their work on open, unrestricted Internet sites or deposit it in an institutional repository when the draft contains a link to the published version at www.ascelibrary.org. "Final draft" means the version submitted to ASCE after peer review and prior to copyediting or other ASCE production activities; it does not include the copyedited version, the page proof, a PDF, or full-text HTML of the published version.

Exceptions to the Copyright Transfer policy exist in the following circumstances. Check the appropriate box below to indicate whether you are claiming an exception:

☐ **U.S. GOVERNMENT EMPLOYEES:** Work prepared by U.S. Government employees in their official capacities is not subject to copyright in the United States. Such authors must place their work in the public domain, meaning that it can be freely copied, republished, or redistributed. In order for the work to be placed in the public domain, ALL AUTHORS must be official U.S. Government employees. If at least one author is not a U.S. Government employee, copyright must be transferred to ASCE by that author.

☐ **CROWN GOVERNMENT COPYRIGHT:** Whereby a work is prepared by officers of the Crown Government in their official capacities, the Crown Government reserves its own copyright under national law. If ALL AUTHORS on the manuscript are Crown Government employees, copyright cannot be transferred to ASCE; however, ASCE is given the following nonexclusive rights: (1) to use, print, and/or publish in any language and any format, print and electronic, the above-mentioned work or any part thereof, provided that the name of the author and the Crown Government affiliation is clearly indicated; (2) to grant the same rights to others to print or publish the work; and (3) to collect royalty fees. ALL AUTHORS must be official Crown Government employees in order to claim this exemption in its entirety. If at least one author is not a Crown Government employee, copyright must be transferred to ASCE by that author.

☐ **WORK-FOR-HIRE:** Privately employed authors who have prepared works in their official capacity as employees must also transfer copyright to ASCE; however, their employer retains the rights to revise, adapt, prepare derivative works, publish, reprint, reproduce, and distribute the work provided that such use is for the promotion of its business enterprise and does not imply the endorsement of ASCE. In this instance, an authorized agent from the authors' employer must sign the form below.

☐ **U.S. GOVERNMENT CONTRACTORS:** Work prepared by authors under a contract for the U.S. Government (e.g., U.S. Government labs) may or may not be subject to copyright transfer. Authors must refer to their contractor agreement. For works that qualify as U.S. Government works by a contractor, ASCE acknowledges that the U.S. Government retains a nonexclusive, paid-up, irrevocable, worldwide license to publish or reproduce this work for U.S. Government purposes only. This policy DOES NOT apply to work created with U.S. Government grants.

I, the corresponding author, confirm that the authors listed on the manuscript are aware of their authorship status and qualify to be authors on the manuscript according to the guidelines above.

I, the corresponding author, confirm that the content, figures (drawings, charts, photographs, etc.), and tables in the submitted work are either original work created by the authors listed on the manuscript or work for which permission to re-use has been obtained from the creator.

I, the corresponding author, acting with consent of all authors listed on the manuscript, hereby transfer copyright or claim exemption to transfer copyright of the work as indicated above to the American Society of Civil Engineers.

Jingjing Liu

Print Name of Author or Agent

Jingjing Liu

数字签名者：Jingjing Liu
DN：cn=Jingjing Liu, o, ou, email=jingjing.liu88@gmail.com, c=CA
日期：2019.04.29 03:44:46 +08'00'

Signature of Author of Agent | Date

NOTE: If you do not wish to sign the form digitally, please print, sign, scan, and email (books) or upload (journals) the form. More information regarding the policies of ASCE can be found in Publishing in ASCE Journals at https://doi.org/10.1061/9780784479018

Additional Requirements:

1. The authors have removed the tables and figures from within the manuscript.
2. The authors have used boldface for matrixes, vectors, tensors; italics for all variables, including variables that are subscript and superscript; roman for all numerals and Greek characters, and mathematical operators; and Helvetica for all dimensionless numbers (Froude, Weber, Prandtl, etc.).

Reviewer #1:

1. It is suggested that the Authors include a reference to recent shake-table testing performed at UC San Diego, which included CLT walls with angle brackets and nailed connections presented in Engineering Structures.

Answer: The reference mentioned above has been addressed in the literature review in Line 25.

van de Lindt, J. W., Furley, J., Amini, M. O., Pei, S., Tamagnone, G., Barbosa, A. R., Rammer, D., Line, P., Fragiacomoi, M., and Popovski, M. (2019). "Experimental seismic behavior of a two-story CLT platform building. " Eng.Struct., 183, 408-422.

2. Line 173 "unloading strength increased" - Revise and potentially clarify what is understood by "unloading strength"

Answer: The authors aimed to point out that the gap size factor β caused significant change of the unloading path from the maximum load to 0 kN force.

Thus, line 172-174 “It was observed that, as the gap size factor decreased, the loading capacity slightly increased. The most significant effect is that the unloading strength increased, and the degradation weakened as β decreased.” were rewritten for more clarification as below,

It was observed that, as the gap size factor decreased, first, the maximum loading capacity slightly increased. Second, the unloading path from the maximum load to 0 kN force changed significantly. Third, the slipping distance between 0 mm displacement and the displacement where the force was unloaded to 0 kN decreased. Finally, the degradation effect was weakened.

3. Line 284 "Similar characters were observed..."

Answer: The sentence has been rewritten as below for clarification:

In Set D, the co-existent shear force weakened the energy dissipation capacity of hold-downs significantly at large vertical displacements, as shown in Fig. 13.

4. Line 295 "The parameters used to calculate those force-displacement curves are presented and discussion as below."

Answer: The sentence has been revised as "The parameters used to calculate the force-displacement curves are presented and **discussed** as below."

5. The terms "method", "methodology", "algorithm" seem to be used interchangeably to describe the HYST model although the three terms mean different things. Please revise throughout the paper. See for example, lines 348 to 352.

Answer: The terms "method", "methodology", "algorithm" have all been revised to "algorithm" throughout the paper to describe the HYST model.

6. The Authors discuss the "original" and "modified" HYST models as developed in Foschi and Yao (2000) and Li et al. (2011), respectively. Would it make for the Authors to "brand" the modifications developed in the paper under review, mainly including the beta and gamma factors and adjustments to the unloading paths, so that it is easier for future readers and users of the implementations to refer to the right version of the HYST model?

Answer: As suggested by the reviewer, the proposed version of the HYST model which mainly including the beta and gamma factors and adjustments to the unloading paths has been “branded” as the "optimized" HYST model, which has been modified throughout the paper.

Reviewer #2: None.